

Article

A Convolutional Fuzzy Neural Network Active Noise Cancellation Approach without Error Sensors for Autonomous Rail Rapid Transit

Tao Li ^{1,2,3,4}, Yuyao He ¹, Minqi Wang ¹, Kaihui Zhao ⁵ , Ning Wang ¹, Weihua Gui ⁶, Jianghua Feng ⁷ and Jun Yang ^{3,*}

- ¹ School of Railway Transportation, Hunan University of Technology, Zhuzhou 412007, China; litao@hut.edu.cn (T.L.); ohuoa1@163.com (Y.H.); wminqi@163.com (M.W.); ningwang5279@163.com (N.W.)
² School of Mechanical and Vehicle Engineering, Hunan University, Changsha 410083, China
³ Zhuzhou Times New Material Technology Co., Ltd., Zhuzhou 412007, China
⁴ Department of Computer Science, The University of Sheffield, Sheffield S10 2TN, UK
⁵ School of Electrical and Information Engineering, Hunan University of Technology, Zhuzhou 412007, China; zhaokaihui@hut.edu.cn
⁶ College of Automation, Central South University, Changsha 410083, China; gwh@csu.edu.cn
⁷ CRRC Zhuzhou Institute Co., Ltd., Zhuzhou 412007, China; fengjh@csrzc.com
* Correspondence: yangjun20012021@163.com

Abstract: Autonomous rail rapid transit (ART) is a new type of multiunit, articulated, rubber-wheeled urban transport system. The noise sources of ART have significant time-varying characteristics. It is unsuitable to track the error signal by installing too many error sensors, which poses a significant challenge in the active noise control of ART. Thus, this paper proposes a convolutional fuzzy neural network-based active noise cancellation approach without error sensors to solve this problem. The proposed approach utilizes convolutional neural network (CNN) to extract the noise signal characteristics of ART and trains multiple noise source signals using a CNN to estimate the virtual error signal in the target area. In addition, the proposed approach adopts fuzzy neural network (FNN) for adaptive adjustment of filter weight coefficients to achieve real-time noise tracking control with fast convergence and small error in the convergence process. The experimental results demonstrate that the proposed approach can effectively reduce ART low-frequency noise without error sensors, and the average sound pressure level in the target area is reduced more compared with conventional approaches.

Keywords: error sensors; convolutional fuzzy neural network; autonomous rail rapid transit; active noise cancellation



Citation: Li, T.; He, Y.; Wang, M.; Zhao, K.; Wang, N.; Gui, W.; Feng, J.; Yang, J. A Convolutional Fuzzy Neural Network Active Noise Cancellation Approach without Error Sensors for Autonomous Rail Rapid Transit. *Processes* **2023**, *11*, 2576. <https://doi.org/10.3390/pr11092576>

Academic Editor: Jiaqiang E

Received: 13 July 2023

Revised: 14 August 2023

Accepted: 20 August 2023

Published: 28 August 2023



Copyright: © 2023 by the authors. Licensee MDPI, Basel, Switzerland. This article is an open access article distributed under the terms and conditions of the Creative Commons Attribution (CC BY) license (<https://creativecommons.org/licenses/by/4.0/>).

1. Introduction

Autonomous rail rapid transit (ART) is a new type of multiunit, articulated, rubber-wheeled urban transport vehicle system that involves more complicated noise sources and more pronounced sound field coupling. Also, an ART vehicle is a large vehicle with a capacity of over 300 passengers per trip. Therefore, the noise of ART is more challenging to control. Effective control of ART noise is essential to improve the comfort of autonomous rail rapid transit. Vehicle noise is an important environmental and social issue because long-term exposure to excessively noisy environments can cause irreversible damage to people's hearing.

Traditional noise control approaches utilize passive noise control techniques such as acoustic absorption and sound insulation to reduce noise. However, these approaches are frequently limited in practical engineering applications due to their size, mass, cost, and low-frequency noise suppression performance. As a result, active noise control (ANC)

approaches have been proposed. ANC approaches use microphones and electronic loudspeakers to generate sound waves with frequencies that are the same as that of the noise source and phases that are opposite to that of the noise source. These are then superimposed in space to produce phase-dissipative interference to weaken the sound energy and reduce the noise [1–4]. Shahin presented general criteria for controlling source and error microphone locations in order to improve the performance of active noise barriers [5].

The most commonly used ANC approach is the simple and easy-to-implement filtered-X least mean square (FXLMS) approach, which can facilitate noise reduction in practical engineering applications such as automobiles [6–9]. However, the FXLMS approach has identifiable limitations, such as an insufficient convergence speed and large mean square error (MSE). Several researchers have proposed the normalized filtered-X least mean square (NFXLMS) approach, which converges the coefficients by normalizing the reference signal power. Thus, the convergence time is independent of the reference signal power [10], which improves the convergence speed. Shi proposed a dual-gradient directional filter-x least mean square (2GD-FXLMS) approach based on the optimal Kuhn–Tucker solution with output constraints. This approach minimizes system overspeed and maintains a certain power budget while improving system stability [11]. Huang et al. proposed the variable step size filtered-x least mean square (VSFXLMS) approach, which varies the step size to take different convergence coefficients. As a result, the final noise reduction effect is balanced between the convergence speed and steady state error [12]. In addition, Li introduced the fractional order concept and implemented a multichannel FXLMS approach, using multiple error sensors and loudspeakers to achieve better performance in terms of reducing noise in a large area [13]. These approaches require a number of error sensors to collect noise in a local zone of quiet (ZoQ) around the target noise reduction area as a feedback signal to the approach [14,15]. However, installing many error sensors for active noise reduction in large-space multiunit ART systems is difficult due to vehicle structure, process, and cost constraints.

In recent years, artificial neural network technology has developed rapidly and has demonstrated advantages in terms of prediction performance and computational costs. Thus, artificial neural network technology is widely used in many fields such as transportation [16–18]. For example, An proposed a approach to predict traffic flow using a fuzzy convolutional neural network (FCNN), which introduces uncertain traffic incident information into the CNN while utilizing a fuzzy approach to represent traffic incident characteristics. With this approach, accurate prediction of Beijing taxi-related data was achieved [19]. To predict driving fatigue effectively, Du proposed a deep learning framework of a TSK-type convolutional recurrent fuzzy network (TCRFN) based on the spatiotemporal characteristics of EEG signals [20], which demonstrated better anti-noise performance and prediction accuracy in a fatigue prediction task. Hepzibah employed a fuzzy approach to remove ambiguities in the input images to enhance the CNN's recognition of road places [21]. Zhou studied a neural network feedforward ANC approach based on the error backpropagation (BP) approach, which has good tracking capability under variation in the original signal [22]. Thus, the properties of neural networks can be considered to predict the error noise signal in the target noise reduction area, thereby realizing ANC for ART without error sensors.

This paper proposes a convolutional fuzzy neural network (C-FNN) active noise cancellation approach without error sensors for ART. The noise signal characteristics are extracted and modeled using the invariance of the convolutional layer in the convolutional network. After training multiple noise signals through the convolutional network, the virtual error signal is fitted and estimated to approximate the real error noise signal in the target area. The FNN is used for offline identification of the secondary pathways during control, and the neural network weight coefficients are adjusted adaptively to achieve fast convergence and small errors in the convergence process and the tracking control process without sensors. Through semi-physical simulation experiments under different simulated noise sources and ART vehicle experiments, we verify that the C-FNN algorithm

without error sensors exhibits a faster convergence speed and better noise reduction effect than the traditional FXLMS algorithm, normalized LMS algorithm, and BP neural network algorithm for ANC.

2. Approach

The advantages offered by CNN and FNN technologies have been combined to develop the C-FNN. Multiple primary noise signals are estimated by fitting a convolution module to obtain an accurate virtual error signal that is close to the real error noise signal, and then the fuzzy module is utilized for online tracking control to improve noise reduction. Compared with the traditional BP neural network, the convolutional network can use the translation invariance of the convolutional layer to deeply extract and model the noise signal characteristics, and simultaneous sharing of the weight can reduce the network's calculation costs and increase the calculation speed [23]. Here, assume that the noise signal picked up by the primary sensors at multiple noise sources is converted to a digital signal as follows:

$$X(n) = [X_1(n), X_2(n), \dots, X_k(n)] \quad (1)$$

In Equation (1), k is the number of primary sensors, n is the number of sensor sampling points in a single run, and $X_k(n)$ is the noise signal picked up by the k th sensor, expanded to

$$X_k(n) = [x_k(n), x_k(n-1), \dots, x_k(n-l)] \quad (2)$$

where l is the sequence length. A sensor can be set up at the target noise reduction point to collect the real noise signal for CNN training, denoted by

$$R(n) = [r(n), r(n-1), \dots, r(n-l)] \quad (3)$$

Note that $X(n)$ is computed iteratively in the convolution and pooling layers, and the estimated virtual error signal $o(n)$ is output through the activation function:

$$o(n) = f\left(\sum X(n) * \omega(n) + b(n)\right) \quad (4)$$

where $f(\cdot)$ is the activation function, $\omega(n)$ is the weight of the convolutional network, and $b(n)$ is the network bias.

To avoid the problem of the commonly used ReLU activation function for CNN models in the negative interval resulting in neurons not learning, the Leaky ReLU function is used as the activation function, which is mathematically represented as follows:

$$f(\theta) = \begin{cases} \theta, & \theta > 0 \\ \theta/a, & \theta \leq 0 \end{cases} \quad (5)$$

where θ is the independent variable of the function and a is a parameter in the interval $(1, +\infty)$. The CNN module training function is defined in Equation (6). Here, the weights and biases are updated according to the training function as shown in Equation (7) and Equation (8):

$$E(n) = 1/2(r(n) - o(n))^2 \quad (6)$$

$$\omega(n+1) = \omega(n) - \eta \frac{\partial(0.5(r(n) - o(n))^2)}{\partial \omega(n)} \quad (7)$$

$$b(n+1) = b(n) - \eta \frac{\partial(0.5(r(n) - o(n))^2)}{\partial b(n)} \quad (8)$$

Using the translational invariance of the convolutional layer in the convolutional network to extract and model the noise signal features, we build the relationship between multiple primary noise signals and the error signal in the target area, and we construct a virtual error signal $o(n)$ rather than the real error sensor in engineering.

The convolutional network output signal $o(n)$ is input to the FNN and uses the FNN for offline identification of the secondary pathways and adaptive tuning of the neural network weight coefficients to achieve fast convergence and small errors in the convergence process without requiring error sensors for tracking control. Here, $o(n)$ is input to the fuzzy layer, which calculates the affiliation value according to the fuzzy rules and activates the affiliation value using the multiplication function, where j is the number of nodes in the fuzzy layer (with a total of H nodes) and μ_j is the affiliation function, expressed as shown in Equation (9):

$$\mu_j(o(n)) = \exp \left[\frac{-(o_j(n) - c_j(n))^2}{\sigma_j^2(n)} \right] \quad (9)$$

Here, $c(n)$ and $\sigma(n)$ are the center and width of the affiliation function, respectively. Finally, the output value of the fuzzy layer is calculated as follows:

$$y(n) = \sum_j^H \mu_j(o(n)) \cdot (p_0 + p_1 o(n)) / \sum_j^H \mu_j(o(n)) \quad (10)$$

where p_0 and p_1 are the fuzzy coefficients. The objective function $J(n)$ of the active noise cancellation approach can be expressed as follows:

$$J(n) = \frac{1}{2} e^2(n) = \frac{1}{2} [d(n) - y'(n)]^2 \quad (11)$$

where $d(n)$ is the desired signal, which is the reference signal passing through the primary path $P(z)$ to the target noise reduction point, and $y'(n)$ is the noise reduction signal obtained by passing the C-FNN output signal $y(n)$ through the secondary path $H(z)$. Here, $d(n)$ and $y'(n)$ are expressed as given in Equations (12) and (13), respectively:

$$d(n) = X(n) * P(z) \quad (12)$$

$$y'(n) = y(n) * H(z) \quad (13)$$

Due to the time-varying nature of the noise signal, the FNN is trained in real time, and the parameters in the network are updated by gradient descent according to the objective function $J(n)$. In other words, the noise cancellation signal $y'(n)$ is infinitely close to the desired signal $d(n)$, and the objective function $J(n)$ is close to zero. The updated equations for each parameter are given in Equations (14)–(16):

$$p(n+1) = p(n) - \alpha \frac{\partial J(n)}{\partial p(n)} \quad (14)$$

$$c(n+1) = c(n) - \beta \frac{\partial J(n)}{\partial c(n)} \quad (15)$$

$$\sigma(n + 1) = \sigma(n) - \beta \frac{\partial J(n)}{\partial \sigma(n)} \tag{16}$$

where α and β are the fuzzy network learning rates. Equations (9) and (10) integrated into Equation (13) can calculate $y'(n)$, which is the noise reduction signal obtained by passing the C-FNN output signal through the secondary path.

$$y'(n) = \sum_j^H \exp \left[\frac{-(o_j(n) - c_j(n))^2}{\sigma_j^2(n)} \right] \cdot (p_0 + p_1 o_j(n)) / \sum_j^H \exp \left[\frac{-(o_j(n) - c_j(n))^2}{\sigma_j^2(n)} \right] * H(z) \tag{17}$$

The C-FNN employs a convolutional layer and a pooling layer to fit multiple noise signals acquired by the primary sensor and estimate the virtual error noise signal $o(n)$ as the input to the fuzzy layer, and then it calculates and outputs the optimal noise cancellation signal $y'(n)$ through adaptive adjustment of the neural network weight coefficients. The structure of C-FNN-based active noise cancellation without error sensors is shown in Figure 1.

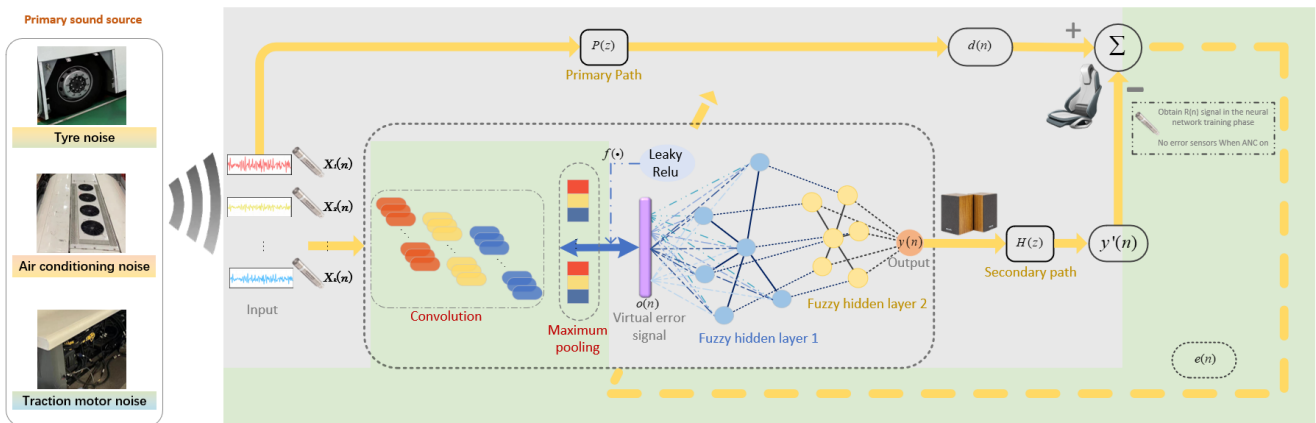


Figure 1. Block diagram of active noise cancellation approach based on convolutional fuzzy neural network without error sensors.

3. Simulation

We constructed an active noise cancellation model based on C-FNN noise prediction in MATLAB. First, we conducted simulation experiments by controlling different simulated noise sources, and then we selected white noise sources for the co-simulation of different approaches to compare and verify the performance of the proposed approach.

3.1. Noise Reduction of Analog Noise Sources

A multi-input single-output ANC system based on a C-FNN was constructed. The C-FNN contains three inputs, four hidden layers, and one output. To maximize the use of the network and reduce computational costs, the four hidden layers in the C-FNN included one convolutional layer, one max pooling layer, and two fuzzy hidden layers. The number of convolution kernels in the convolution layer was set to 25, and the size was 3. In addition, the learning rate was set to $\eta = 1 \times 10^{-4}$, $\alpha = 0.5$, and $\beta = 0.01$ according to prior experience. To accelerate the convergence of the C-FNN, the input signals were normalized to map all input signal data to the range of 0–1. The conversion function is given as follows:

$$x^* = \frac{x - \min}{\max - \min} \tag{18}$$

To verify the influence of noise prediction on the control signal, the control effects were compared between two cases. The first case involved directly controlling the calculated output signal without noise prediction, and the second case involved predicting and then controlling the noise signal. The white noise signal was selected as the noise signal, and the simulation results are shown in Figure 2. In addition, different approaches that first predict and then control the noise signal were co-simulated to verify the performance of the proposed C-FNN, and the performance comparison is shown in Figure 3.

As shown in Figure 2a, for both cases, the residual noise was small. However, the directly controlled residual noise tended to become larger in the later stage of convergence, and the residual noise was larger. Compared with Figure 2b, we observed that the ANC system based on the C-FNN was more stable.

Figure 3 shows a performance comparison of different neural networks. The proposed C-FNN applied to active noise cancellation exhibited smaller errors and was more stable than the BP and radial basis function (RBF) networks. Figure 3b shows that in the range of 0–200 Hz, the three networks reduced noise effectively. However, the BP and RBF networks failed to continue to reduce noise thereafter. The proposed C-FNN reduced noise continuously and exhibited a good noise cancellation effect.

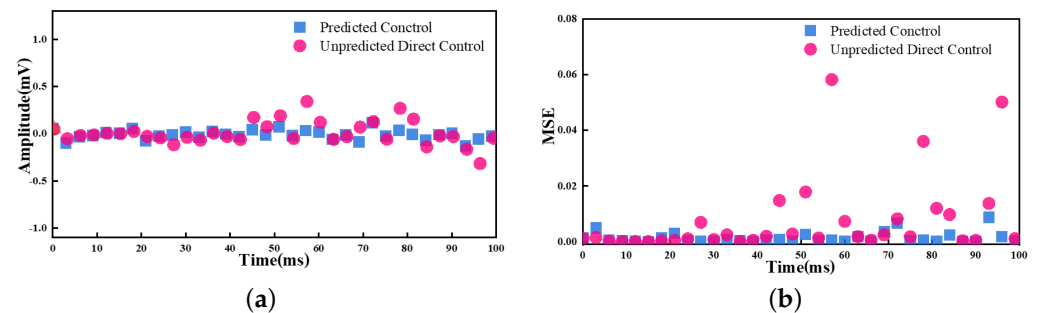


Figure 2. Comparison of direct control and predictive control simulation: (a) residual noise and (b) MSE.

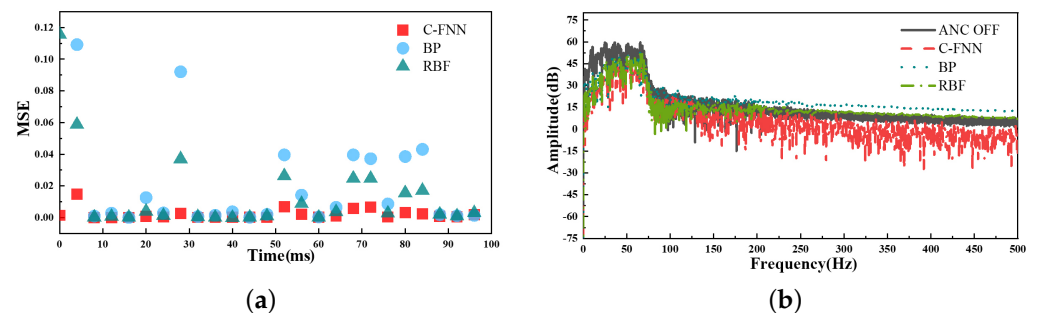


Figure 3. Co-simulation of different neural networks: (a) MSE and (b) spectrogram.

3.2. Semiphysical Simulation

To verify the response characteristics of the proposed ANC system based on a C-FNN to actual noise, we collected noise signals from different parts of ART. Three sensors were arranged in various locations of the cabin to collect noise as the primary noise signals, and the noise signal collected at the seat of the cabin was used as the noise signal for model prediction training. The collected ART noise signal was input to the C-FNN-based active noise cancellation system, and a before-and-after noise reduction diagram is shown in Figure 4.

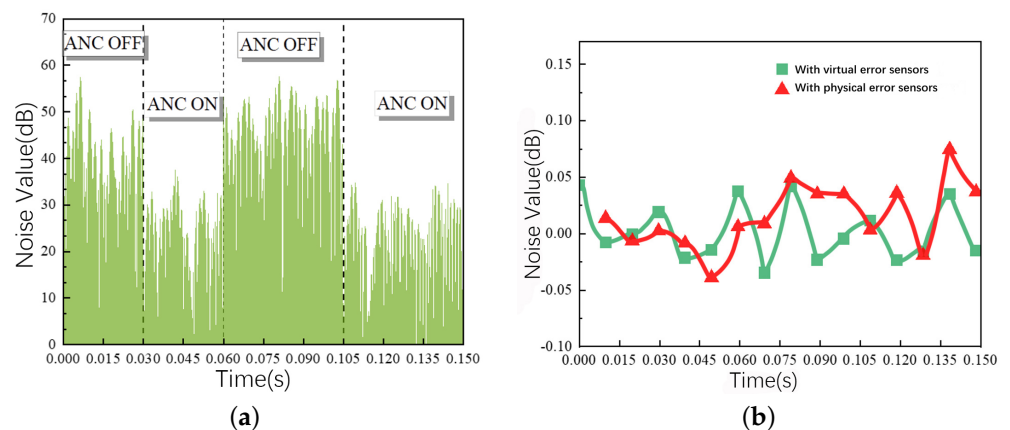


Figure 4. Co-simulation of different neural networks: (a) before and after ANC control and (b) residual noise signal comparison.

Figure 4a shows that after the ANC was turned on, the noise signal could be reduced rapidly by an average of 27.15 dB. Figure 4b shows a comparison of the residual noise. As can be seen, the residual noise was controlled quite well with a virtual error sensor and with a physical sensor, and in the last stage of control, the C-FNN with virtual error sensors approach had even less residual noise than the conventional approach with physical error sensors. This demonstrates that the noise signal controlled by the C-FNN was more stable and better controlled.

4. Experiment

The active noise cancellation system based on the proposed C-FNN approach was designed with LabVIEW, and an experiment was conducted to verify the noise reduction effect of the proposed approach. In this experiment, the control object was noise in the driver's cabin of an ART vehicle.

4.1. Driver's Cabin Noise Analysis of ART

Active noise cancellation based on the C-FNN approach was applied to driver's cabin noise in the ART system, which is an emerging mode of transport that uses artificial intelligence to solve modern urban transport challenges. Unlike conventional rail vehicles, ART utilizes virtual tracks on the ground that use special materials and induction markings buried in the road. Figure 5 shows the ART system in Zhuzhou, including the distribution of air conditioning noise, tire noise, hinge noise, and traction motor noise.

The ART track is a virtual track. Thus, the system has no wheel-track noise. Noise associated with an ART vehicle primarily comprises traction, pneumatic, and road noises. A professional sound level meter was utilized to collect the ART driver's cabin noise. The noise characteristics are shown in Figure 6. As can be seen, the main contribution frequency band of the ART driver's cabin noise was between 80 and 1600 Hz, and low- and medium-frequency noise was evident. Thus, for the driver's cabin noise, active noise cancellation techniques that are applicable to low- and medium-frequencies can be used to control noise.

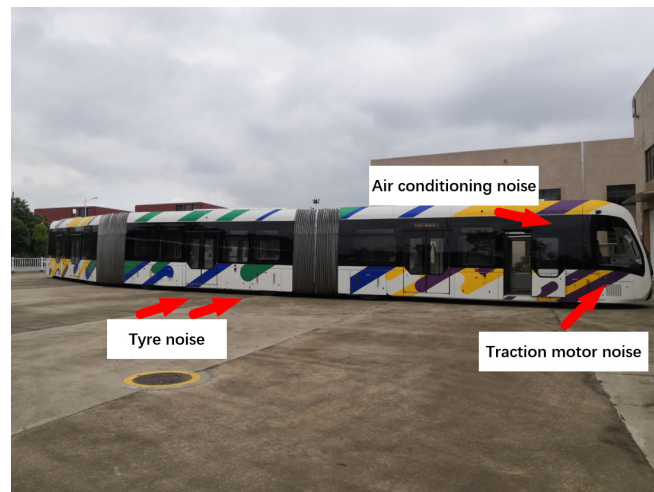


Figure 5. Exterior view of autonomous rail rapid transit vehicle and noise distribution.

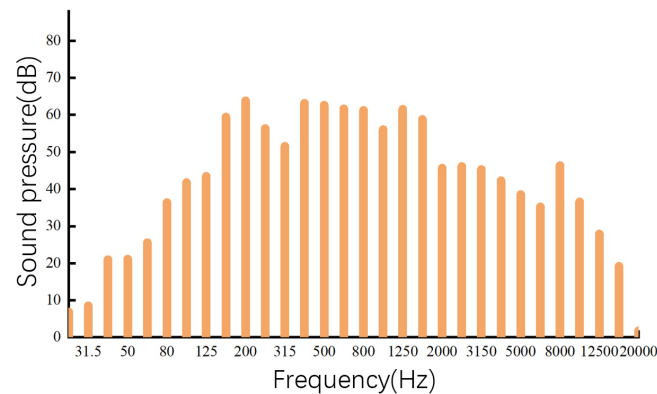


Figure 6. Autonomous rail rapid transit driver's cabin noise (1/3 octave).

4.2. ANC Experiment for ART

The C-FNN-based active noise cancellation system used the following equipment and instruments. The acoustic transducer was a CY-405 sound sensor, which was connected to an NI-cDAQ Ethernet chassis through a Megasig-PM0043 signal conditioner.

In the construction of the proposed approach, an NI cDAQ-9189 Ethernet chassis was used as the controller to run the C-FNN approach, and NI-9215 and NI-9263 boards were configured with analog inputs and outputs.

The experimental process is summarized as follows. The primary sensor collected the noise signal from the primary source, converted it to a digital signal using the NI-9215 analog input module, and transmitted it to the controller. Afterward, the upper computer equipped with LabVIEW calculated the approach of the noise offset signal transmitted to the NI-9263 analog output module converted it to an analog signal through the secondary source playback.

Experiments for noise reduction without error sensors were conducted in the ART driver's cabin. The initial noise signal was collected by three primary microphones. In the neural network training phase, a fourth microphone was used to acquire the signal from the target noise reduction point as a training target for the convolutional network. In the ANC control phase, the fourth microphone test sensor acquired the signal from the target noise reduction point to record the noise reduction effect of the ANC system. Figure 7 shows the experimental equipment of the active noise cancellation approach based on a C-FNN without error sensors for autonomous rail rapid transit.

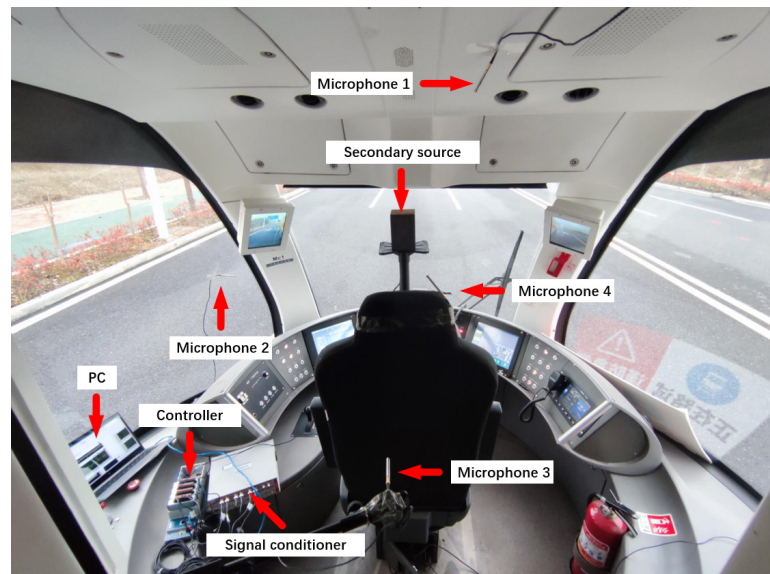


Figure 7. Experimental equipment of active noise cancellation approach based on a C-FNN without error sensors for autonomous rail rapid transit.

The C-FNN parameters were set as $\eta = 1 \times 10^{-7}$, $\alpha = 0.5$, and $\beta = 0.01$. The controller parameters were adjusted to the optimum value, and the sampling rate was set to a maximum of 1 KHz due to the performance of the upper computer (an overly high sampling rate would cause data overflow problems).

During the neural network training phase, the convolutional layer in the convolutional network was used to extract and model the noise signal features. The three primary microphones were placed at the three noise sources to collect the standard primary noise of the noise sources under different working conditions. For example, the main noise sources (tire noise, fan noise, motor noise, etc.) can be collected at different rotation speeds, such as 50 rpm, 100 rpm, and 200 rpm. In addition, a training microphone was placed at the target noise cancellation area to collect the noise, and then all collected noise was input to the CNN for training and continuous iterative operation to obtain the prediction model of the target area.

During the ANC control phase, three primary microphones were placed at each of the three noise sources to collect noise in real time, and a single test microphone was placed at the target noise cancellation area to test the noise cancellation effect. This experiment began with the ART vehicle driving on the road, and the noise collected in real time was input to the trained CNN model to obtain an estimate of the real-time noise in the target area. The estimated results were then combined with the estimated noise calibrated by the trained model to obtain the virtual error noise signal, which was then used as feedback for the FNN. The FNN was utilized to identify the secondary pathways offline, and the neural network weight coefficients were adjusted adaptively to obtain the noise cancellation signal $y'(n)$, which was played out through the secondary source to achieve fast convergence and a small error value in the convergence process of the ANC without error sensors. The results are shown in Figure 8.

In Figure 8a, the solid blue line is the noise signal at the target noise cancellation area collected by the fourth microphone, and the red dashed line is the obtained virtual error signal $o(n)$. As can be seen, the calculated virtual error signal $o(n)$ generally fit the noise signal collected by the fourth microphone. Figure 8b shows the error between the virtual error signal $o(n)$ and the noise signal at the target noise cancellation area. As can be seen, the error was between -1 and 1 dB (i.e., the primary noise signal was strongly correlated with the noise signal at the target noise cancellation area).

Figure 8c shows the noise cancellation results in the time domain. We observe that the noise cancellation effect was good, except for the noise increase at individual points,

with an average sound pressure level cancellation of approximately 2.2 dB and a maximum of 8.2 dB. Figure 8d shows the results in the frequency domain. As shown, there was significant noise cancellation (up to 18 dB) near the 150 Hz and 260 Hz peaks.

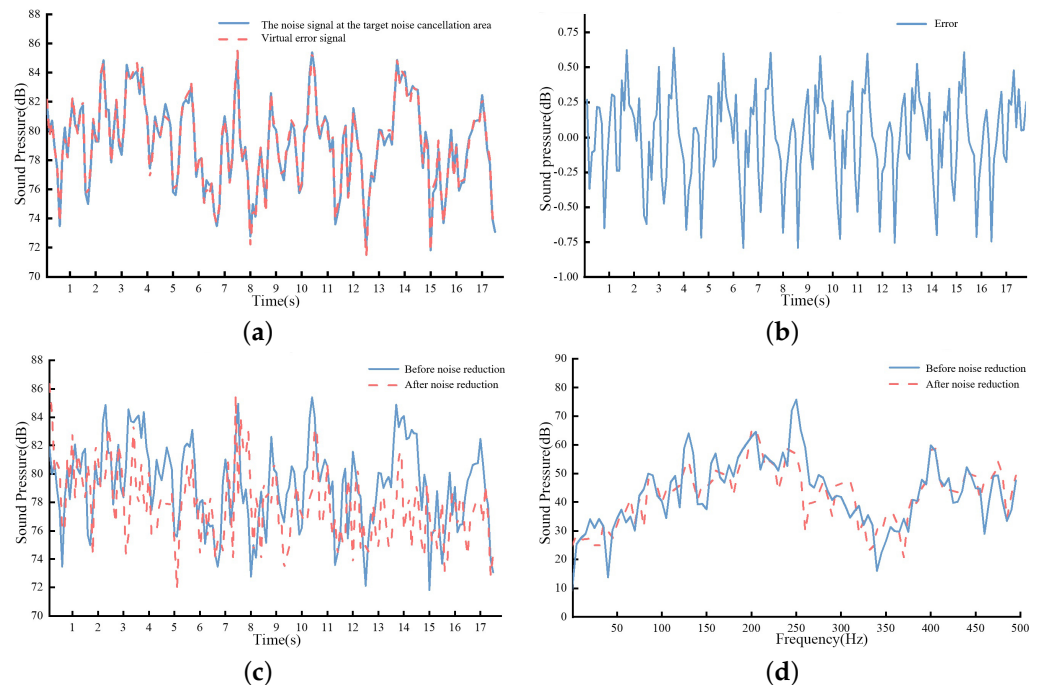


Figure 8. The results of the active noise cancellation experiment in autonomous rail rapid transit driver's cabin. (a) Fitting of the virtual error signal. (b) The difference between the noise signal at the target noise cancellation area and the virtual error signal. (c) Time domain analysis of noise reduction effects. (d) Frequency domain analysis of noise reduction effects.

To further verify the effectiveness of the proposed approach, the convolutional fuzzy neural network ANC approach without error sensors and traditional ANC approaches with error sensors were compared and analyzed in noise reduction experiments under three ART operating conditions: smooth running, acceleration, and deceleration. Typical traditional ANC approaches with error sensors include normalized LMS (N-LMS) and FXLMS. In the experiments involving traditional approaches, the primary sensor picked up the source noise as the reference signal, and the error sensors picked up the noise at the noise reduction target as the error signals.

Figure 9a,b shows the time and frequency domain analyses of the noise at the noise reduction point during smooth operation of the ART system. Orange indicates the noise without the noise reduction system, purple indicates the noise reduction of the ANC system without the error sensors, green indicates the noise reduction of the ANC system with the error sensors based on the N-LMS approach, and blue indicates the noise reduction of the ANC system with the error sensors based on the FXLMS approach.

In Figure 9a, during smooth operation of the ART system, the noise decreased by 7 dB for the active noise cancellation system without the error sensor noise, by 6.8 dB for the active noise cancellation system with the error sensor based on the N-LMS approach, and by 4.5 dB for the active noise cancellation system with the error sensor based on FXLMS. Compared with the active noise cancellation system without the error sensor noise, the N-LMS and FXLMS approaches with the error sensor noise cancellation system exhibited jitter amplitudes of approximately 6.3 dB and 4 dB in the early control period, respectively.

Similarly, as shown in Figure 9c, during the accelerated operation of the ART system, the noise decreased by 8.2 dB for the active noise cancellation system without the error sensor noise, by 7.6 dB for the active noise cancellation system with the error sensor based on the N-LMS approach, and by 5 dB for the active noise cancellation system with the error

sensor based on the FXLMS approach. Compared with the active noise cancellation system without the error sensor noise, the N-LMS and FXLMS approaches with the error sensor noise cancellation system showed jitter amplitudes of approximately 5 dB and 2.2 dB in the early control period, respectively.

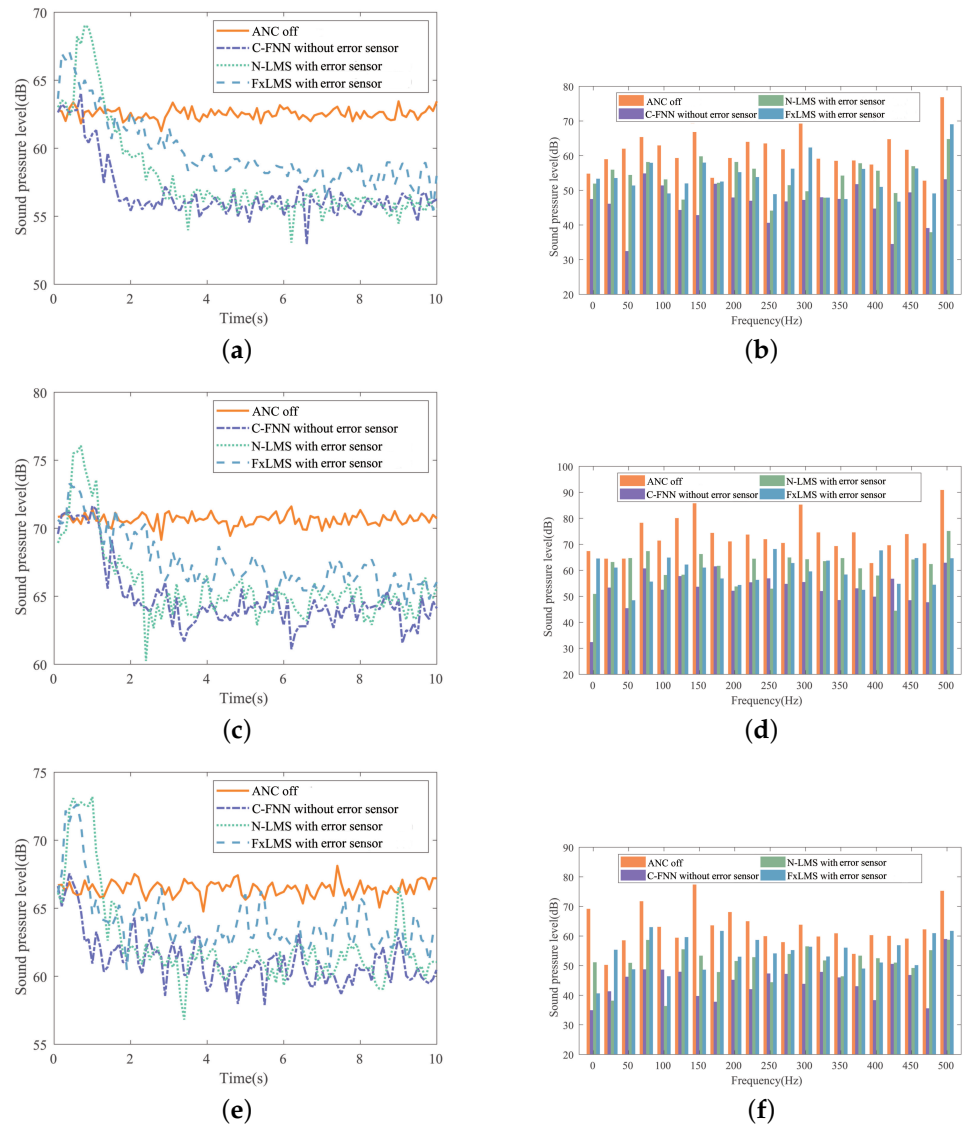


Figure 9. The noise reduction effects of the active noise cancellation system with an error sensor compared with one without the error sensor. (a) Time domain analysis under smooth operating conditions of ART vehicle. (b) Frequency domain analysis under smooth operating conditions of ART system. (c) Time domain analysis under acceleration operating conditions of ART system. (d) Frequency domain analysis under acceleration operating conditions of ART system. (e) Time domain analysis under deceleration operating conditions of ART vehicle. (f) Frequency domain analysis under deceleration operating conditions of ART system.

Figure 9e shows that during the deceleration operation of the ART system, the noise decreased by 6.5 dB for the active noise cancellation system without the error sensor, by 6 dB for the active noise cancellation system with the error sensor based on the N-LMS approach, and by 3.8 dB for the active noise cancellation system with the error sensor based on the FXLMS approach. Compared with the active noise cancellation system without the error sensor noise, N-LMS and FXLMS with the error sensor noise cancellation system exhibited jitter amplitudes of approximately 7 dB and 10 dB in the early control period, respectively.

Figure 9b,d,f shows that, compared with the active noise cancellation system with the error sensor noise, the noise reduction effect of the active noise cancellation system without the error sensor noise was the best in most of the frequency domain (from 0 to 500 Hz), and its average noise cancellation effect was superior to the compared noise cancellation systems.

In summary, the data-driven nonlinear active noise control without error sensors was more fault-tolerant in such large spaces with high levels of interference. Compared with the active noise cancellation approach with error sensors, the proposed approach demonstrated obvious advantages in the ART noise cancellation experiments. The superiority of the noise cancellation effect can be observed from the time and frequency domains. In addition, the proposed approach reduces the use of sensors. Thus, it has high engineering applicability.

5. Conclusions

This paper proposed an active noise cancellation approach without sensors based on a C-FNN. This approach approximates the true error noise signal in the target area by training multiple noise signals and uses a CNN to fit and estimate the virtual error signal. During the control process, the secondary pathways are identified offline by the FNN, and the weight coefficients of the neural network are adaptively adjusted. Finally, the approach with an error sensor achieved fast convergence and small error values in the convergence process.

The simulation results demonstrate that the proposed approach without error sensors can track noise signals quickly and reduce and stabilize the residual noise efficiently. The co-simulation of different neural networks demonstrated that the proposed approach is more stable and causes less residual noise than the traditional ANC approach with error sensors.

In an active noise cancellation experiment conducted in an ART system, the proposed approach effectively controlled the ART system's low-frequency noise. Compared with the active noise cancellation approach with error sensors, the proposed approach exhibits advantages under different operating conditions, such as smooth speed, acceleration, and deceleration of the ART vehicle. Our findings demonstrate that the proposed approach reduces dependence on error sensors, which is expected to contribute to active noise cancellation applications for large vehicles such as those in ART systems.

Author Contributions: Conceptualization, T.L.; methodology, T.L. and Y.H.; software, M.W. and Y.H.; validation, M.W., Y.H. and N.W.; formal analysis, J.Y.; investigation, W.G.; resources, J.F.; data curation, T.L. and K.Z.; writing—original draft preparation, Y.H.; writing—review and editing, M.W.; visualization, N.W.; supervision, W.G.; project administration, J.F.; funding acquisition, J.Y. All authors have read and agreed to the published version of the manuscript.

Funding: This work was supported in part by the National Natural Science Foundation of China under Grants 62173137 and 52172403, in part by the Natural Science Foundation of Hunan Province under Grant 2020JJ6067, and in part by the Scientific Research and Innovation Foundation of Hunan University of Technology (CX2011).

Data Availability Statement: Not applicable.

Conflicts of Interest: The authors declare no conflict of interest. The funders had no role in the design of the study; in the collection, analyses, or interpretation of data; in the writing of the manuscript; or in the decision to publish the results.

References

1. Lam, B.; Shi, D.; Gan, W.S.; Elliott, S.J.; Nishimura, M. Active control of broadband sound through the open aperture of a full-sized domestic window. *Sci. Rep.* **2020**, *10*, 10021. [[CrossRef](#)] [[PubMed](#)]
2. Shi, D.; Lam, B.; Gan, W.S.; Wen, S. Block coordinate descent based algorithm for computational complexity reduction in multichannel active noise control system. *Mech. Syst. Signal Process.* **2021**, *151*, 107346. [[CrossRef](#)]
3. Samarasinghe, P.N.; Zhang, W.; Abhayapala, T.D. Recent advances in active noise control inside automobile cabins: Toward quieter cars. *IEEE Signal Process. Mag.* **2016**, *33*, 61–73. [[CrossRef](#)]

4. Zhou, C.; Zou, H.; Qiu, X. A frequency band constrained filtered-x least mean square algorithm for feedback active control systems. *J. Acoust. Soc. Am.* **2020**, *148*, 1947–1951. [[CrossRef](#)] [[PubMed](#)]
5. Sohrabi, S.; Pàmies Gómez, T.; Romeu Garbí, J. Proper location of the transducers for an active noise barrier. *J. Vib. Control.* **2023**, *29*, 2290–2300. [[CrossRef](#)]
6. Song, P.; Zhao, H. Filtered-x least mean square/fourth (FXLMS/F) algorithm for active noise control. *Mech. Syst. Signal Process.* **2019**, *120*, 69–82. [[CrossRef](#)]
7. Chen, J.; Yang, J. A distributed FxLMS algorithm for narrowband active noise control and its convergence analysis. *J. Sound Vib.* **2022**, *532*, 116986. [[CrossRef](#)]
8. Zhang, S.; Zhang, L.; Meng, D.; Pi, X. Active control of vehicle interior engine noise using a multi-channel delayed adaptive notch algorithm based on FxLMS structure. *Mech. Syst. Signal Process.* **2023**, *186*, 109831. [[CrossRef](#)]
9. Wang, H.; Zhang, J.; Gan, L.; Liu, Y. Directional Suppression of Monotone Noises with A Parametric Array Loudspeaker. *Appl. Sci.* **2023**, *13*, 6868. [[CrossRef](#)]
10. Yin, W.; Wei, Y.; Liu, T.; Wang, Y. A novel orthogonalized fractional order filtered-x normalized least mean squares algorithm for feedforward vibration rejection. *Mech. Syst. Signal Process.* **2019**, *119*, 138–154. [[CrossRef](#)]
11. Shi, D.; Gan, W.S.; Lam, B.; Shi, C. Two-gradient direction FXLMS: An adaptive active noise control algorithm with output constraint. *Mech. Syst. Signal Process.* **2019**, *116*, 651–667. [[CrossRef](#)]
12. Rajagopal, R.; Palanisamy, K.; Paramasivam, S. Comparative performance of normalized LMS and variable step size LMS based control for shunt active filtering. In Proceedings of the 2019 9th International Conference on Advances in Computing and Communication (ICACC), Kochi, India, 6–8 November 2019; pp. 136–141.
13. Li, T.; Wang, M.; He, Y.; Wang, N.; Yang, J.; Ding, R.; Zhao, K. Vehicle engine noise cancellation based on a multi-channel fractional-order active noise control algorithm. *Machines* **2022**, *10*, 670. [[CrossRef](#)]
14. Mylonas, D.; Erspamer, A.; Yiakopoulos, C.; Antoniadis, I. An extrapolation-based virtual sensing technique of improving the control performance of the FxLMS algorithm in a maritime environment. *Appl. Acoust.* **2022**, *193*, 108756. [[CrossRef](#)]
15. Shi, D.; Lam, B.; Wen, S.; Gan, W.S. Multichannel active noise control with spatial derivative constraints to enlarge the quiet zone. In Proceedings of the ICASSP 2020–2020 IEEE International Conference on Acoustics, Speech and Signal Processing (ICASSP), Virtual, 4–9 May 2020; pp. 8419–8423.
16. Li, T.; He, Y.; Wang, N.; Feng, J.; Gui, W.; Zhao, K. Active Noise Cancellation of Rail Vehicles Based on a Convolutional Fuzzy Neural Network Prediction Approach. In Proceedings of the 2021 IEEE Vehicle Power and Propulsion Conference (VPPC), Virtual, 25 October–14 November 2021; pp. 1–5.
17. Ziółkowski, J.; Oszczypta, M.; Małachowski, J.; Szkutnik-Rogoż, J. Use of artificial neural networks to predict fuel consumption on the basis of technical parameters of vehicles. *Energies* **2021**, *14*, 2639. [[CrossRef](#)]
18. Dong, Z.; Wu, Y.; Pei, M.; Jia, Y. Vehicle type classification using a semisupervised convolutional neural network. *IEEE Trans. Intell. Transp. Syst.* **2015**, *16*, 2247–2256. [[CrossRef](#)]
19. An, J.; Fu, L.; Hu, M.; Chen, W.; Zhan, J. A novel fuzzy-based convolutional neural network method to traffic flow prediction with uncertain traffic accident information. *IEEE Access* **2019**, *7*, 20708–20722. [[CrossRef](#)]
20. Du, G.; Wang, Z.; Li, C.; Liu, P.X. A TSK-type convolutional recurrent fuzzy network for predicting driving fatigue. *IEEE Trans. Fuzzy Syst.* **2020**, *29*, 2100–2111. [[CrossRef](#)]
21. Hepzibah, J.; Kalaiselvi, S.; Anitha, V.; Gomathi, V. Road segmentation from remote sensing images using fuzzy based convolutional neural network. In Proceedings of the AIP Conference Proceedings, Kovilpatti, India, 14–15 May 2021; AIP Publishing LLC: New York, NY, USA, 2022; Volume 2444, p. 040007.
22. Zhou, Y.L.; Zhang, Q.Z.; Li, X.D.; Gan, W.S. Analysis and DSP implementation of an ANC system using a filtered-error neural network. *J. Sound Vib.* **2005**, *285*, 1–25. [[CrossRef](#)]
23. Park, S.; Patterson, E.; Baum, C. Long Short-Term Memory and Convolutional Neural Networks for Active Noise Control. In Proceedings of the 2019 5th International Conference on Frontiers of Signal Processing (ICFSP), Marseille, France, 18–20 September 2019; pp. 121–125.

Disclaimer/Publisher’s Note: The statements, opinions and data contained in all publications are solely those of the individual author(s) and contributor(s) and not of MDPI and/or the editor(s). MDPI and/or the editor(s) disclaim responsibility for any injury to people or property resulting from any ideas, methods, instructions or products referred to in the content.